Cell Chemical Biology

Degradome analysis to identify direct protein substrates of small-molecule degraders

Graphical abstract

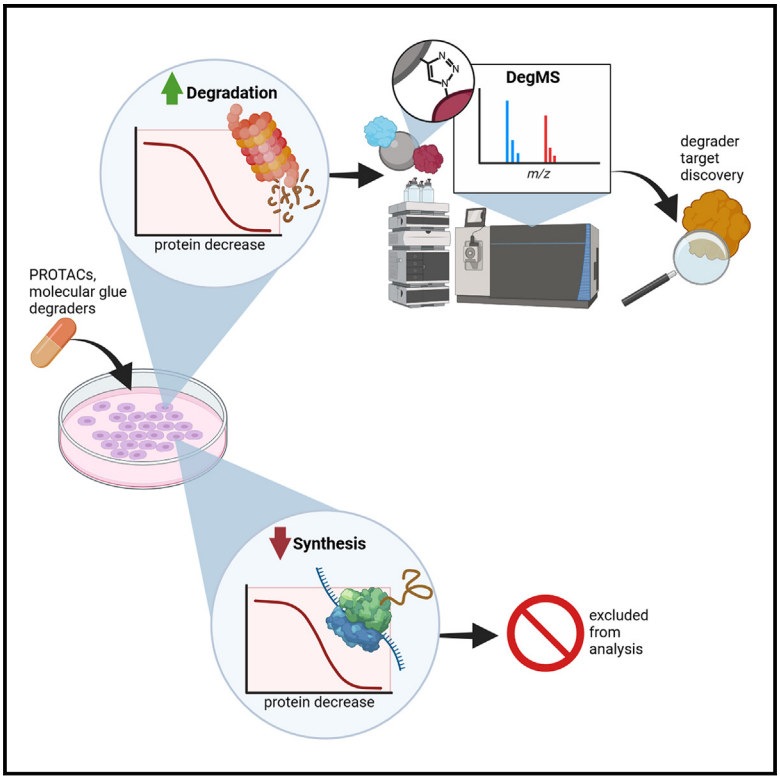

Highlights

- DegMS selectively investigates treatment-induced protein degradation
- Target identification of protein degraders during short or prolonged drug exposure
- Not affected by compensatory cellular effects via transcription or translation
- Target identification of an uncharacterized molecular glue degrader

Authors

Marco Jochem, Anna Schrempf, Lina-Marie Wagner, ..., Amanda Ng, Georg E. Winter, Jeroen Krijgsveld

Correspondence

j.krijgsveld@dkfz.de

In brief

Jochem et al. present DegMS, a proteomic approach to selectively investigate protein degradation that combines stable isotope-labeling, click-chemistry, and mass spectrometry. Resilience to compensatory cellular effects enables substrate identification of protein degraders during short or prolonged drug exposure with high specificity, as shown for known and uncharacterized molecular glue degraders.

Jochem et al., 2025, Cell Chemical Biology *32*, 192–200
January 16, 2025 © 2024 The Author(s). Published by Elsevier Ltd.
https://doi.org/10.1016/j.chembiol.2024.10.007

CellPress
OPEN ACCESS

Cell Chemical Biology

Technology

Degradome analysis to identify direct protein substrates of small-molecule degraders

Marco Jochem,[1] Anna Schrempf,[2] Lina-Marie Wagner,[1] Dmitri Segal,[2] Jose Cisneros,[2] Amanda Ng,[2] Georg E. Winter,[2] and Jeroen Krijgsveld[1,3,4,*]
[1]German Cancer Research Center (DKFZ), Heidelberg, Germany
[2]CeMM Research Center for Molecular Medicine of the Austrian Academy of Sciences, 1090 Vienna, Austria
[3]Heidelberg University, Medical Faculty, Heidelberg, Germany
[4]Lead contact
*Correspondence: j.krijgsveld@dkfz.de
https://doi.org/10.1016/j.chembiol.2024.10.007

SIGNIFICANCE Small-molecule degraders are an emerging class of drugs that act by directing their target protein for degradation. This contrasts with conventional drugs that inhibit the activity of their target, thereby offering new therapeutic options. However, a remaining challenge is to unambiguously identify the direct substrate of such degraders, and to distinguish this from proteins that change in abundance due to an indirect cellular response to drug treatment. Here we introduce an approach to investigate perturbation-induced protein degradation at a proteomic scale, termed DegMS, by combining pulse labeling of cellular proteins with stable isotopes, click chemistry, and MS. We demonstrate that DegMS can monitor protein degradation at a timescale that is compatible with the activity of small-molecule degraders. In addition, DegMS negates confounding effects of altered transcription and translation induced by target depletion, thus contributing to its high specificity. We show the strength of DegMS in the identification of substrates of known degraders, and by characterizing the target of an uncharacterized molecular glue. This positions DegMS as a powerful approach for substrate discovery in the emerging field of TPD.

SUMMARY

Targeted protein degradation (TPD) has emerged as a powerful strategy to selectively eliminate cellular proteins using small-molecule degraders, offering therapeutic promise for targeting proteins that are otherwise undruggable. However, a remaining challenge is to unambiguously identify primary TPD targets that are distinct from secondary downstream effects in the proteome. Here we introduce an approach for selective analysis of protein degradation by mass spectrometry (DegMS) at proteomic scale, which derives its specificity from the exclusion of confounding effects of altered transcription and translation induced by target depletion. We show that the approach efficiently operates at the timescale of TPD (hours) and we demonstrate its utility by analyzing the cyclin K degraders dCeMM2 and dCeMM4, which induce widespread transcriptional downregulation, and the GSPT1 degrader CC-885, an inhibitor of protein translation. Additionally, we apply DegMS to characterize a previously uncharacterized degrader, and identify the zinc-finger protein FIZ1 as a degraded target.

INTRODUCTION

Small-molecule degraders are a category of drugs that exploit the ubiquitin machinery by recruiting E3 ligases to target proteins of interest for their ubiquitination and subsequent degradation by the proteasome.[1–3] This mechanism is very different from traditional drugs that bind and inhibit their targets at functional sites, and therefore targeted protein degradation (TPD) is a promising therapeutic strategy particularly in cases where achieving specificity and druggability has proven challenging. In addition, small-molecule degraders offer advantageous pharmacodynamics, benefiting from their catalytic mode of action that obviates continued target engagement. Moreover, substrate degradation neutralizes both the enzymatic and scaffolding functions of their targets and might hence offer a more profound perturbation. Clinically approved examples of small-molecule degraders are found within the immunomodulatory imide drug (IMiD) family, including thalidomide and its analogs lenalidomide and

 © 2024 The Author(s). Published by Elsevier Ltd.
This is an open access article under the CC BY-NC-ND license (http://creativecommons.org/licenses/by-nc-nd/4.0/).

CellPress
OPEN ACCESS

pomalidomide.[4–6] IMiDs bind to the E3 ligase CRBN and thereby recruit the zinc finger transcription factors IKZF1 and IKZF3, causing their ubiquitination and ensuing degradation by the proteasome. Of note, IMiDs have been successfully used to treat blood cancers such as multiple myeloma. Additionally, numerous small-molecule degraders currently undergo clinical trials, targeting a wide range of proteins, such as androgen and estrogen receptor, BCL-XL, IRAK4, STAT3, BTK, TRK, BRD9, IKZF1/2/3, and GSPT1.[7,8]

Based on their chemical structure and mechanism of action, small-molecule degraders can be divided into two major classes: proteolysis targeting chimeras (PROTACs) and molecular glues.[9] PROTACs are bifunctional molecules composed of two warheads that selectively bind to the E3 ligase and the protein of interest, respectively, connected by a flexible linker. This approach offers a high degree of synthetic flexibility due to the large number of different possible combinations of warheads. In contrast, molecular glues enhance direct protein-protein interactions between the E3 ligase and the target protein to either boost the ubiquitination of existing substrates or enable the ubiquitination and degradation of neo-substrates.[10,11] Molecular glues are typically smaller in size than PROTACs, making them more amenable to pharmacological administration; however, their rational design is complicated by the fact that target engagement is difficult to predict, usually necessitating complex screening strategies to identify novel compounds.[12–14]

Since small-molecule degraders act at the protein level, proteomic methods have become essential to identify their targets and to determine target specificity. Liquid chromatography mass spectrometry (LC-MS) based methods employing label-free or tandem mass tag (TMT)-based multiplexing strategies are routinely used to identify drug-induced proteomic changes without requiring prior knowledge of the drug's targets.[15–17] However, in the context of TPD, conventional global proteomics approaches face the challenge of distinguishing proteins that are degraded as direct drug targets from those that are downregulated due to indirect downstream effects, illustrated by the observation that many drugs alter overall proteome composition.[18] This can be expected especially when targeting transcriptional or translational regulators, which complicates the identification of direct drug targets and inflates the number of candidates that need to be validated independently, as we noted in our own work.[13]

To overcome these challenges, we introduce a proteomics workflow tailored to selectively analyze drug-induced protein degradation while excluding proteomic alterations that arise from indirect transcriptional and translational effects. We apply this degradome strategy to characterize direct targets of established and uncharacterized protein degraders.

DESIGN

Development of DegMS for drug-induced degradome analysis

To identify direct targets of TPD, we developed a strategy termed DegMS that specifically monitors protein degradation by mass spectrometry (MS), and which allows the investigation of protein degradation at a proteomic scale (i.e., degradomics) (Figure 1A; Method S1). DegMS involves (1) the labeling of cells with azidohomoalanine (AHA, a clickable methionine analog) and stable isotope labeling by amino acids in cell culture (SILAC), (2) cell treatment with a small-molecule degrader of interest, and (3) click-chemistry-based protein enrichment followed by MS for the enrichment, identification and quantification of proteins that are depleted from the labeled protein pool. In more detail, SILAC-intermediate-labeled cells are exposed to AHA and either SILAC-light or SILAC-heavy amino acids for an 8-h pulse period. This creates a pool of labeled proteins across the proteome whose abundance is monitored after switching cells back to SILAC-intermediate media, while simultaneously adding a protein degrader or vehicle-treatment (to SILAC-heavy and SILAC-light labeled cells, respectively). Subsequently, AHA-containing proteins are enriched from the labeled pool using click-chemistry and identified and quantified by MS. Crucially, proteins that are newly synthesized after drug addition do not incorporate AHA and differ in their SILAC label status (intermediate). Hence, these proteins are not enriched and can otherwise be distinguished from SILAC-heavy and SILAC-light proteins originating from the labeled protein pool. Therefore this design effectively uncouples drug-induced effects on protein synthesis and degradation, and allows for the selective study of protein degradation that excludes secondary transcriptional and translational effects that may occur after drug administration, as a consequence of target (or off-target) degradation.

RESULTS

Benchmarking of DegMS by target identification of dCeMM2

We reasoned that this degradomics approach should be ideally placed to identify direct targets of TPD. To test this, we applied DegMS to investigate the small-molecule degrader dCeMM2, which we previously discovered through a screening approach for molecular glue degraders,[13] and which targets cyclin K and its interaction partners, the transcriptional kinases CDK12 and CDK13 (Figure 1B). Given that the degradation of cyclin K, CDK12, and CDK13 leads to widespread transcriptional downregulation of other genes,[13] dCeMM2 provided an ideal test case to evaluate the performance of our approach. We pulse-labeled human KBM7 cells, added the drug, and sampled cells at 6 time points during an 8-h time course treatment. Upon digestion of AHA-enriched proteins we observed a noticeable decrease in peptide yield with prolonged drug treatment (Figure 1C), which is expected since no newly synthesized proteins can incorporate AHA, yet all proteins in the AHA-labeled pool progressively undergo both basal and drug-induced degradation. As anticipated, SILAC-intermediate labeled peptides represented by far the smallest fraction of all peptides after enrichment (Figure 1D), demonstrating the efficacy of the workflow in excluding proteins synthesized before and after the 8-h SILAC-AHA pulse period. dCeMM2-induced proteome effects were quantified from SILAC-heavy/SILAC-light ratios, revealing that degradation of the intended target cyclin K occurred already after 1 h of drug treatment, followed by the degradation of CDK12 and CDK13 after 4 h (Figure 1E; Data S1). This degradation kinetics of cyclin K and CDK12/13 fits with their topological engagement in the ternary complex with the E3 ligase.[19] Crucially, these three targets of dCeMM2 were the only downregulated proteins throughout the treatment time course among 4,000–7,000 identified proteins,

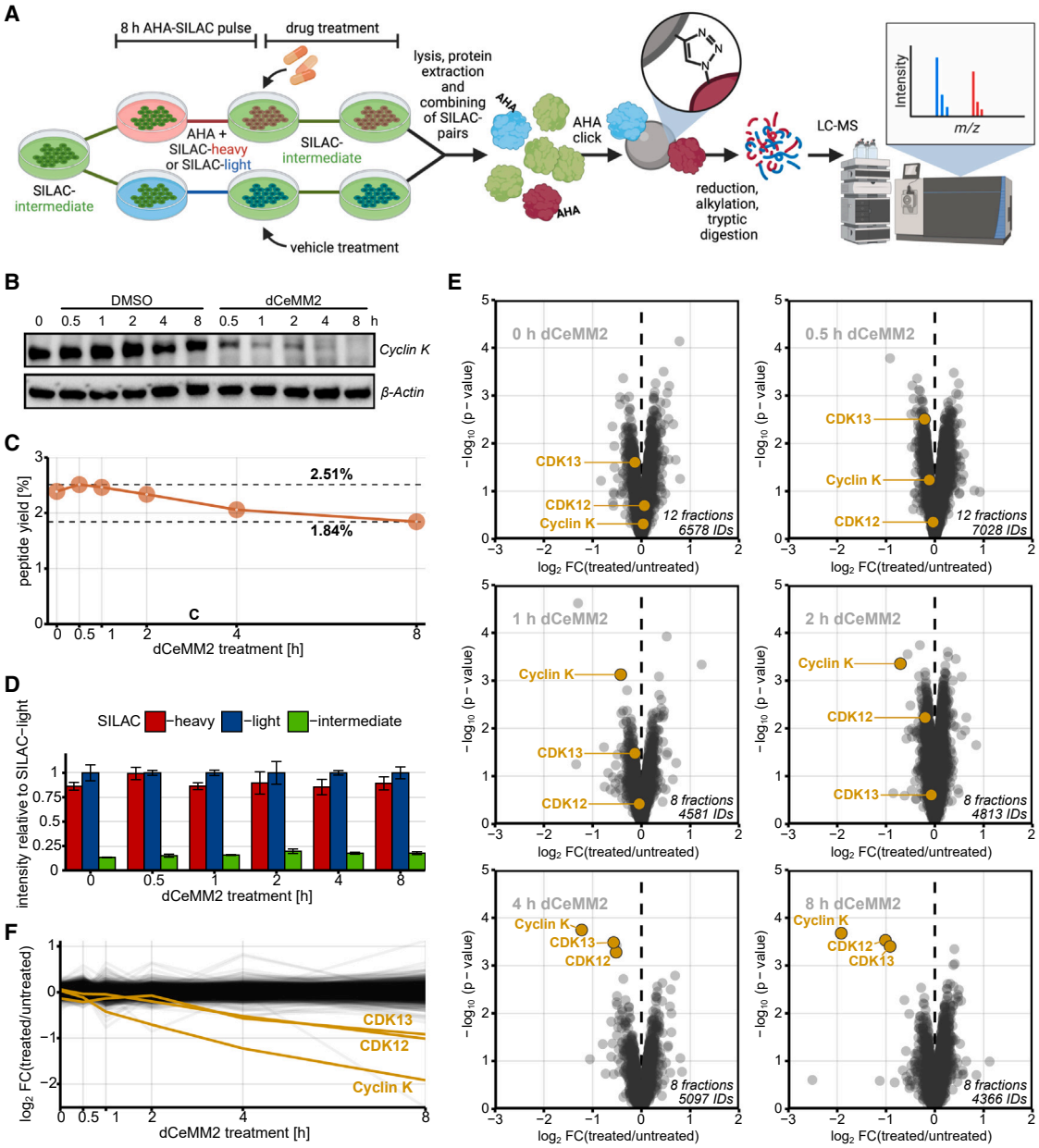

Figure 1. Degradome proteomics by DegMS

(A) Workflow scheme: Fully SILAC-intermediate labeled cells are pulse-labeled with both AHA and SILAC-heavy or SILAC-light amino acids for 8 h. The media is changed back to SILAC-intermediate, and the former heavy-channel is treated with the drug of interest, while the former light-channel is mock-treated. Cells are lysed, proteins extracted, and the corresponding SILAC-channels combined. The pulsed proteins are enriched for AHA via click-chemistry, reduced, alkylated, and digested by trypsin. The resulting peptides are analyzed by LC-MS/MS for protein identification and quantification to determine drug-induced protein degradation inferred from heavy-over-light SILAC-ratios.

(B) Degradation of cyclin K in response to dCeMM2 determined by immunoblot analysis. KBM7 cells were either treated with 2.5 μM dCeMM2 or with DMSO for the indicated time intervals. Upper panel: anti-cyclin K antibody. Lower panel: anti-β-actin (loading control).

(C) Peptide yields after enriching 1.2 mg of protein for AHA while performing degradome proteomics. KBM7 cells were treated with 2.5 μM dCeMM2 or DMSO for 0, 0.5, 1, 2, 4, or 8 h. Protein and peptide yields were monitored via BCA-assay.

(D) Summed peptide intensities of each SILAC-channel relative to the corresponding SILAC-light channel. Error bars represent standard errors of the means.

(E) Volcano plots (log2 protein fold change vs. nominal *p* values) showing differential protein stabilities in response to dCeMM2 treatment at the indicated time points. Highlighted are the three known targets of dCeMM2: cyclin K, CDK12 and CDK13.

(F) Line plot visualizing global protein stabilities over the dCeMM2 time course. Note that each line represents one protein and that only proteins quantified in all time points are shown.

CellPress
OPEN ACCESS

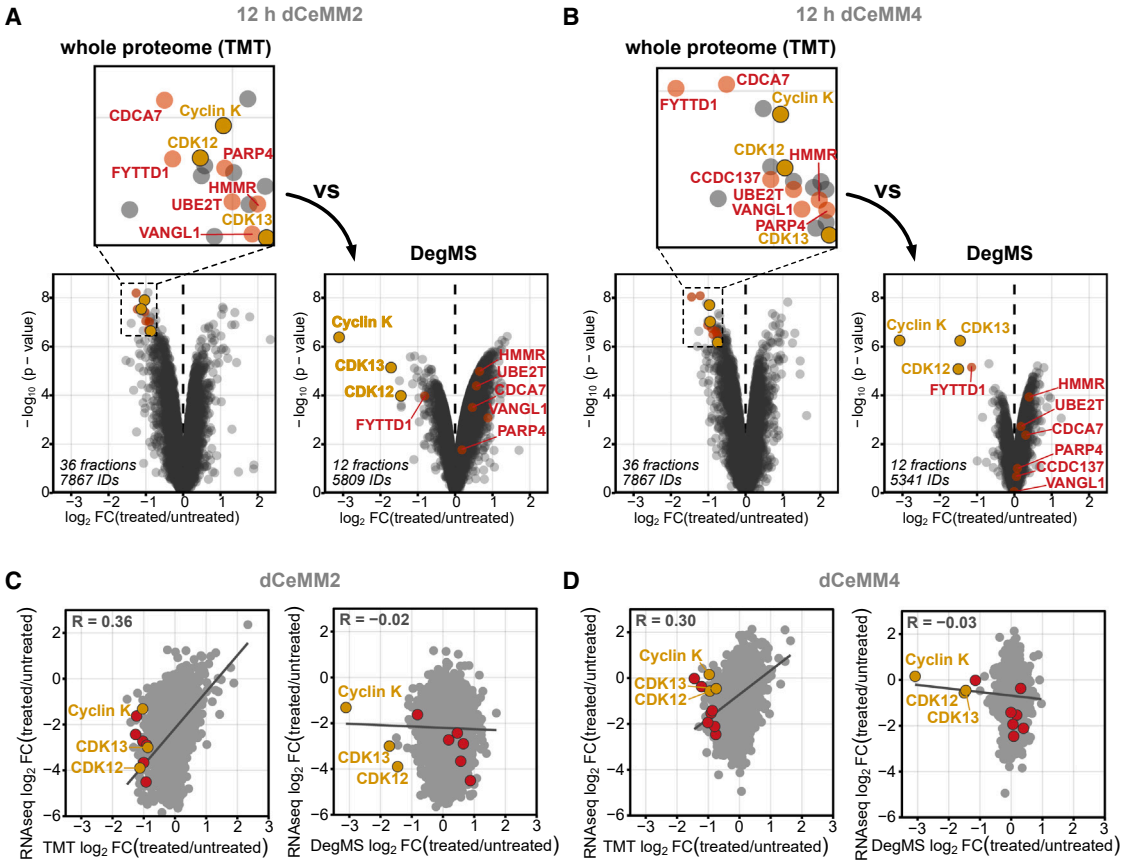

Figure 2. Benchmarking of degradome proteomics by DegMS

(A and B) Comparing degradome proteomics (right) with TMT-based whole proteome analysis (left) for cyclin K degraders. The zoomed-in regions indicate the top-regulated proteins in the TMT-based data, whose distribution is shown in the volcano plot of the degradome data. KBM7 cells were treated with dCeMM2 (2.5 μM) or dCeMM4 (3.5 μM) for 12 h in both approaches. Whole proteome data were taken from Mayor-Ruiz et al.[13] Volcano plots show log2 protein fold change vs. nominal *p* values. Highlighted in yellow are the known degradation targets of dCeMM2 and dCeMM4: cyclin K, CDK12 and CDK13.

(C and D) Pearson correlation between the transcriptome and the whole proteome or the degradome of dCeMM2- and dCeMM4-treated cells. The treatment time for the whole proteome and the degradome analysis was 12 h. The treatment time for the transcriptome analysis was 5 h. See also Figure S1.

indicating the ability of the workflow to selectively identify degradation targets of small molecule degraders (Figure 1F).

We next compared the performance of DegMS with commonly used global proteomic methods, both at an early time point to assess target identification after short drug exposure, and in particular at a later time point when secondary effects may accumulate that mask direct targets. Using a label-free proteome analysis of KBM7 cells upon short (4 h) treatment with dCeMM2 revealed a decrease in abundance of cyclin K; however, without a concomitant change in CDK12 and 13 (Figure S1B; Data S2), thus contrasting with DegMS (Figure 1E). In addition, various other proteins decrease to a similar or even greater extent than cyclin K (Figure S1B), denoting false positives or indirect targets that are absent in DegMS. These data show that DegMS identified targets of dCeMM2 at an earlier time point and with greater specificity. Next, we performed a DegMS experiment in which cells were treated with dCeMM2 and dCeMM4 for 12 h, and we compared the results with data previously obtained using a TMT-based approach under otherwise identical conditions[13] (Figures 2A, 2B, and S1A; Data S3). While several proteins were downregulated in the TMT-dataset along with cyclin K, CDK12 and CDK13, virtually no off-targets were observed in the corresponding degradome dataset. In fact, using DegMS, we found that the three primary targets of dCeMM2 and dCeMM4 almost exclusively ranked at the very top of degraded proteins, while the false-positives in the TMT-approach tended to be stabilized rather than degraded (indicated in red in Figures 2A and 2B). A notable exception was the mRNA export adaptor FYTTD1/UIF, which both proteomics approaches detected as downregulated in response to both drugs, signifying it as another target of degradation. Interestingly, FYTTD1 was previously determined to be a Nedd8-dependent substrate of Cullin-RING ubiquitin ligases,[20] and it was identified as an off-target of both the BET-degrader JQ-1 (leading to downstream arrest in protein synthesis[21]) and of a CDK9 degrader acting via the E3 ligase KEAP1.[22]

Many of the proteins that exhibited significant downregulation in the whole proteome dataset were also downregulated at the transcript level (Figures S1B and S1C, RNA-seq data from Mayor-Ruiz et al.[13]). We even observed a positive correlation between the transcriptome and whole proteome for both dCeMM2- and dCeMM4-treated cells (R = 0.36 and R = 0.3),

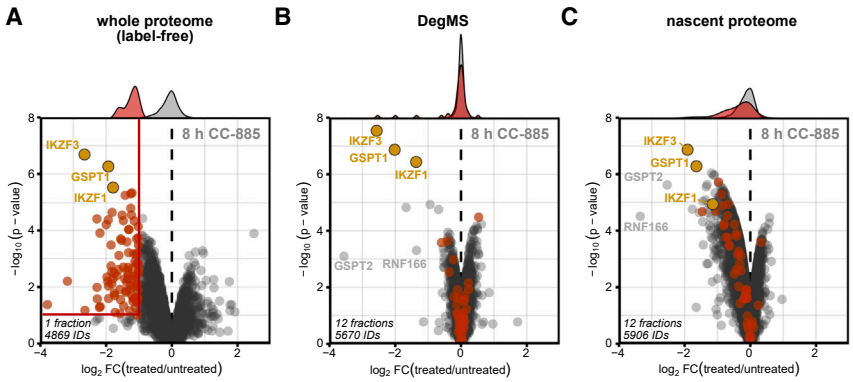

Figure 3. Proteome response to CC-885 treatment

(A) Label-free whole proteome, (B) degradome, and (C) nascent proteome analysis for GSPT1 degrader CC-885. Jurkat cells were treated with 100 nM CC-885 for 8 h in all three approaches. Volcano plots show log2 protein fold change vs. nominal *p* values. Highlighted in yellow are three known targets of CC-885, and in red all proteins that were downregulated in the whole proteome dataset ($\log_2$FC (treated/untreated) < −1 and $-\log_{10}$(*p*-value) > 1). See also Figure S2.

indicating that a substantial portion of drug-induced proteome changes was driven by transcriptional regulation (Figures 2C and 2D). In contrast, the degradome dataset showed no correlation with the transcriptome data (R = −0.02 and R = −0.03), underscoring that our approach is not confounded by such secondary effects.

DegMS efficiently identifies the translational regulator GSPT1 as a target of CC-885

We next turned to CC-885, a pleiotropic molecular glue degrader from the IMiD family that targets the small GTPase GSPT1.[23] Since GSPT1 (also called eRF3 for eukaryotic release factor 3) functions by interacting with the translation termination factor eRF1 to mediate protein translation, CC-885 treatment leads to extensive remodeling of the proteome, masking GSPT1 among multiple other downregulated proteins.[24] Reflecting this challenge to distinguish direct from indirect targets, in fact GSPT1 was originally identified as a substrate of CC-885 by affinity pull-down of tagged CRBN, not by global proteomics.[23] To evaluate whether DegMS could lead to a more unambiguous identification of direct CC-885 targets by negating secondary effects caused by GSPT1 depletion, we conducted side-by-side analyses of different proteomic methods on CC-885-treated cells. Analyzing the whole proteome via label-free data independent acquisition (DIA)-MS, we observed the downregulation of numerous proteins, including the anticipated targets GSPT1, IKZF1, and IKZF3 (Figure 3A; Data S4). This sharply contrasted with degradome analysis by DegMS, where GSPT1, IKZF1, and IKZF3 stood out as the prime targets, while the other proteins that were downregulated in the global proteome were not affected (Figure 3B; Data S4). Interestingly, an approach for nascent proteome analysis that we developed previously to selectively label and enrich for newly synthesized proteins[25] (for experimental scheme see Figure S2), showed that CC-885 treatment induced a profound and global downregulation of proteins, including those observed in the global proteome, as well as GSPT1, IKZF1, and IKZF3 (Figure 3C; Data S4), consistent with a generic role of GSPT1 in translation termination. Additionally, the degradome and the nascent proteome approaches identified the downregulation of the GSPT1-homolog GSPT2, which has been previously found as a target of CC-885,[24] and the E3 ubiquitin ligase RNF166, observed as an off-target of several IMiDs.[26,27] Collectively, these data show the ability of DegMS to identify direct substrates of TPD even if they have a profound role in regulating proteome homeostasis, such as GSPT1.

Identification of FIZ1 as the target of an uncharacterized IMiD

Next, we used DegMS to characterize the previously disclosed IMiD-based degrader compound 1, yet whose targets are unknown (Figure 4A).[28] Upon treatment of Jurkat cells with compound 1, three common IMiD targets were among the most prominently degraded proteins, including IKZF1 and IKZF3 (Figure 4B; Data S5), as confirmed by western blot (Figure 4C), and ZFP91 (Figure 4B).[27,29] Collectively this indicates that we accessed the expected target space. In addition, we observed the degradation of FIZ1 (Flt3-interacting zinc finger protein 1), which, like many other IMiD targets, is a zinc finger-containing protein, but which to our knowledge has not been previously described as a substrate of other small-molecule degraders. FIZ1 plays a role in FMS-like receptor tyrosine kinase 3 (FLT3) signaling,[30,31] functions as a transcriptional repressor,[32,33] and is associated with pro-proliferative effects in keratinocytes.[34] We confirmed the compound 1-induced degradation of FIZ1 through immunoblot analysis in both HEK293T and Jurkat cells (Figures 4D and 4E). Furthermore, we demonstrated via luminescence assay that the rate of degradation is dose-dependent (Figure 4F). In line with a CRBN-dependent mechanism of action, we observed that the compound 1-induced degradation of FIZ1 was impeded when inhibiting the proteasome, ubiquitination, or neddylation, (Figure 4G), while this was rescued upon knock-out of CRBN (Figure 4H). Collectively, this establishes FIZ1 as a genuine TPD target of compound 1. Investigating an extended panel of IMiDs, we found that both pomalidomide and CC-90009 are also capable of degrading FIZ1 (Figure 4I) in a CRBN-dependent manner (Figure 4H). In conclusion, degradome analysis by DegMS efficiently identifies direct targets of small-molecule degraders by monitoring drug-induced protein decay, while negating secondary proteome effects induced by target depletion. Thereby, this fills an important need for target identification of novel protein degraders.

DISCUSSION

In this study, we have introduced and validated a proteomics-based workflow designed to selectively identify targets of

CellPress
OPEN ACCESS

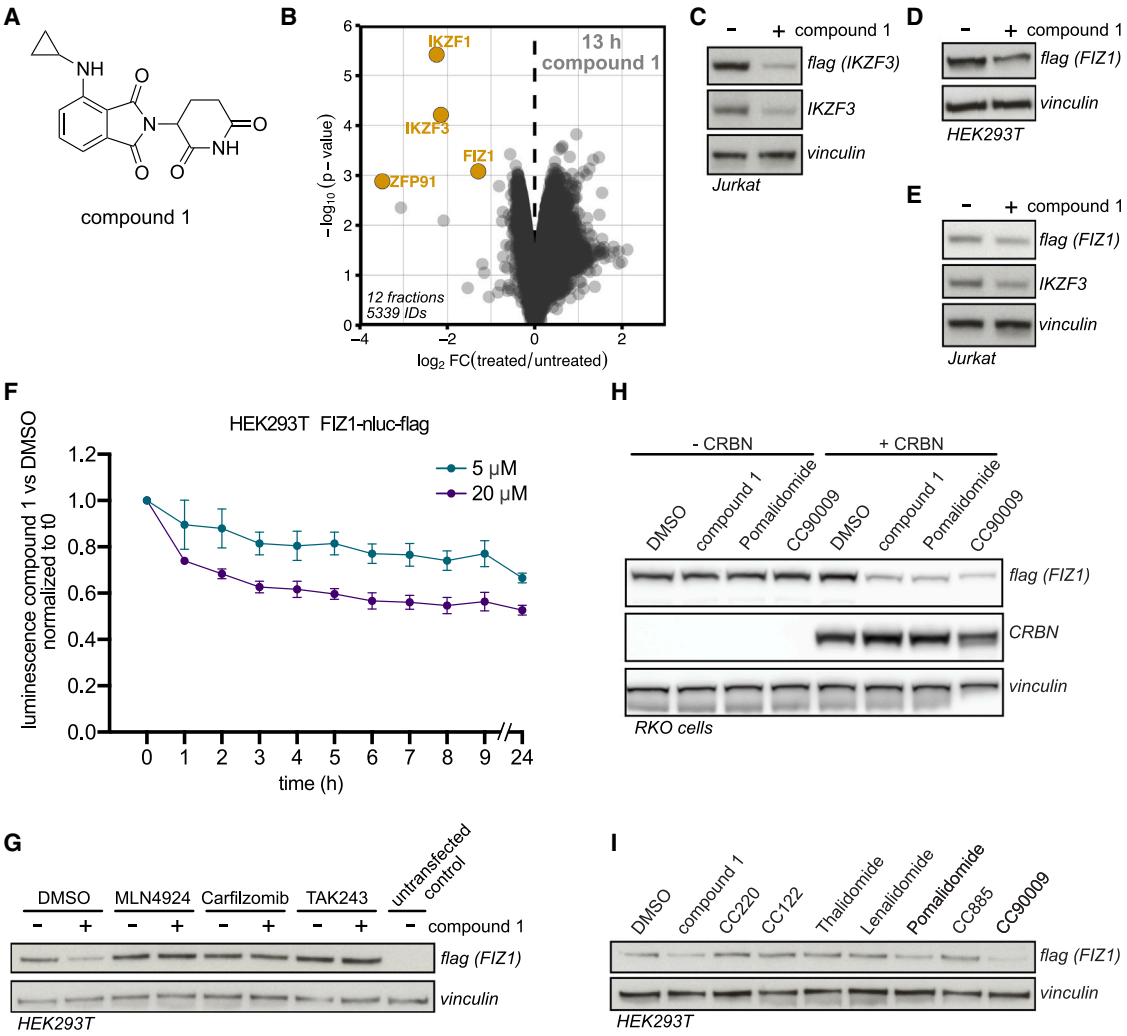

Figure 4. Validation of FIZ1 as a degradation target of compound 1

(A) Chemical structure of small molecule degrader compound 1.

(B) Volcano plot of degradome proteomics under compound 1 treatment (log2 protein fold change vs. nominal *p* values). Jurkat cells were treated for 13 h with 5 μM compound 1 or DMSO. Downregulated proteins are highlighted in yellow.

(C) Degradation of IKZF3-nluc-FLAG and endogenous IKZF3 in response to compound 1 treatment determined by immunoblot analysis. Jurkat cells were treated with 10 μM compound 1 or DMSO for 15 h. Antibodies used: anti-FLAG, anti-IKZF3, and anti-vinculin (loading control).

(D and E) Degradation of FIZ1-nluc-FLAG in response to compound 1 treatment determined by immunoblot analysis in (D) Hek293T cells and (E) in Jurkat cells. Cells were treated with 10 μM compound 1 or DMSO for 16 h. Antibodies used: anti-FLAG, anti-IKZF3 (positive control), and anti-vinculin (loading control).

(F) Luminescence assay in HEK293T cells treated with either compound 1 (5 μM, 20 μM) or DMSO for the indicated times. Error bars represent standard errors of the mean.

(G) Degradation of FIZ1-nluc-FLAG in response to 20 μM compound 1 treatment for 13 h in HEK293T cells under inhibition of neddylation (1 μM MLN4924 = NAE inhibitor), the proteasome (1 μM carfilzomib) or ubiquitination (10 μM TAK243 = UBA1 inhibitor), determined by immunoblot analysis. Upper panel: anti-FLAG antibody. Lower panel: anti-vinculin (loading control).

(H) Degradation of FIZ1-nluc-FLAG in the presence and absence of CRBN. Monoclonal CRBN knockout RKO cells with and without reconstituted wild-type CRBN and transduced with a lentiviral plasmid for stable expression of FIZ1-NanoLuc-3xFLAG were treated with DMSO or 10 μM of compound 1, CC-90009, or pomalidomide for 24 h.

(I) Degradation of FIZ1-nluc-FLAG in response to different small molecule degraders determined by immunoblot analysis. HEK293T cells were treated with DMSO, 20 μM compound 1, 10 μM CC220, 10 μM CC122, 10 μM thalidomide, 10 μM lenalidomide, 10 μM pomalidomide, 10 μM CC-885, or 10 μM CC-90009 for 15 h.

small-molecule protein degraders. A key feature of our approach is that it decouples the drug-induced effects on protein synthesis and degradation, allowing the latter to be analyzed without confounding effects of the former. This is achieved by the incorporation of a SILAC and AHA pulse period prior to drug treatment, which creates an isolated protein pool whose decay can be monitored without being affected by altered protein translation resulting from subsequent depletion of TPD targets. Unlike conventional whole proteome analyses and pulse-chase experiments to monitor protein decay under steady-state conditions,[35]

our method is purpose-built to discern acute perturbation-induced changes in protein stability, and it is therefore tailored to the target-discovery of protein degraders. We showed its efficacy by identifying targets of known degraders (CeMM2, CeMM4, and CC-885), even if their targets themselves impact proteome homeostasis (cyclin K and GSPT1; Figures 2A, 2B, and 3). Although analysis of nascent proteins has been proposed as a method to identify TPD targets,[29] we demonstrated that direct analysis of protein degradation led to more unambiguous target identification while negating secondary effects in the proteome (Figures 3B and 3C). Moreover, we establish that degradome analysis by DegMS operates at the rapid timescale of TPD (hours; Figure 1E), offering the possibility to limit duration of drug treatment and further minimize the risk of capturing secondary effects. Since GSPT1 degraders are tested in various clinical trials, degradome analysis may be part of such programs to evaluate drug specificity.

DegMS can be applied to virtually any cell line or even primary cells, facilitated by the commercial availability of drop-out media lacking Met, Arg, and Lys as used in this study. We labeled cells with SILAC and AHA for 8 h throughout our studies; however, this may need some adaptation especially for cells with a long doubling time to achieve sufficient label incorporation across the proteome. We envision that the utility of DegMS extends to other areas of TPD research, e.g., using autophagy targeting chimeras (AUTACs)[36] and lysosome targeting chimeras (LYTACs).[37] Even more generally, it may be used to the study of protein stability in various other biological contexts; e.g., in autophagic and lysosome-mediated processes. Conversely, the recruitment of deubiquitinases (DUBs) to other proteins through DUB-targeting chimeras (DUBTACs) can lead to their targeted stabilization (TPS), another novel therapeutic concept that is especially relevant in pathologies that are driven by excessive protein degradation.[38] Although not specifically assessed here, we anticipate that DegMS has the capacity to measure drug-induced protein stabilization as well. Our method also has the potential to assist in the identification of endogenous substrates of E3 ligases, which is important for drug development but has proven challenging.[39]

Limitations of the study

Obtaining broad proteome coverage in the pool of labeled proteins is critical for an unbiased analysis of protein degradation in DegMS: a protein that is not labeled during the pulse exposure to AHA and SILAC amino acids will escape detection in subsequent steps, with the potential consequence that true TPD substrates may be missed or indirect targets underestimated. In this study, we pulse-labeled for 8 h (Figure 1A) to generate 4,500–7,000 quantified proteins (Figures 1E, 2A, 2B, 3, and 4B). Although this always included the expected target(s), in principle this number can be increased by extending the labeling time. This cannot be done indefinitely (e.g., to label the entire proteome) since cells poorly tolerate prolonged exposure to AHA, but a labeling time of up to 24 h has been successfully used in other applications.[40] Although we did not test exhaustively here, we found 8 h as an adequate balance between proteome coverage and potential adverse effects of AHA. Proteome coverage may be further enhanced by using a more sensitive mass spectrometer than the instrument used in this study. Currently, a bottleneck of our method resides in the use of off-line peptide fractionation, a time-intensive and laborious process that was used here to achieve comprehensive proteome coverage in data-dependent acquisition (DDA). However, we anticipate that this step can be omitted with the emergence of DIA optimized for SILAC-labeled proteins.[41] In fact, we have recently implemented such an approach in combination with a semi-automated workflow to perform AHA-based protein enrichment for the investigation of perturbation-induced effects on protein translation.[42] The prospect of automated degradome analyses presents an exciting opportunity to develop a powerful tool tailored for high-throughput drug screening in TPD research.

RESOURCES AVAILABILITY

Lead contact

Further information and requests for resources and reagents should be directed to and will be fulfilled by the lead contact, Jeroen Krijgsveld (j.krijgsveld@dkfz.de).

Materials availability

This study did not generate new unique reagents.

Data and code availability

- All data reported in this paper will be shared by the lead contact upon request. The mass spectrometry proteomics data have been deposited to the ProteomeXchange Consortium via the PRIDE repository[43] (http://www.proteomexchange.org) and are publicly available as of the date of publication with the dataset identifier PXD048931.
- This paper does not report original code.
- Any additional information required to reanalyze the data reported in this paper is available from the lead contact upon request.

ACKNOWLEDGMENTS

This work was funded in part by the Deutsche Krebshilfe (project 70114190) (to J.K.). CeMM and the Winter Lab are supported by the Austrian Academy of Sciences. The Winter lab is supported by funding from the European Research Council (ERC) under the European Union's Horizon 2020 research and innovation program (grant agreement 851478), as well as by funding from the Austrian Science Fund (FWF, projects P32125 and P7909). We thank Dimitris Papageorgiou and Wolfgang Huber for advice in statistical analysis. Figures 1A and S2 were created with biorender.com.

AUTHOR CONTRIBUTIONS

Conceptualization: M.J. and J.K.; formal analysis: M.J., A.S., and L.-M.W.; funding acquisition: J.K. and G.E.W.; investigation: M.J., A.S., L.-M.W., and D.S.; methodology: M.J. and J.K.; resources: J.C. and A.N.; supervision: J.K. and G.E.W; writing – original draft: M.J. and J.K; writing – review and editing: G.E.W., A.S., and L.-M.W.

DECLARATION OF INTERESTS

G.E.W. is scientific founder and shareholder of Proxygen and Solgate. The Winter lab received funding from Pfizer.

CellPress
OPEN ACCESS

STAR★METHODS

Detailed methods are provided in the online version of this paper and include the following:

- KEY RESOURCES TABLE
- EXPERIMENTAL MODEL AND STUDY PARTICIPANT DETAILS
  - Cell culture
- METHOD DETAILS
  - Lentivirus production and generation of stable cell lines
  - Small-molecule degraders
  - Synthesis of compound 1
  - Western blot
  - Luminescence assay
  - Pulsed-SILAC-AHA labeling for degradome analysis
  - Pulsed SILAC-AHA labeling for translatome analysis
  - Click-iT protein enrichment, reduction, alkylation and digestion
  - High-pH reversed-phase fractionation
  - DDA-MS for degradome and translatome analysis
  - Sample preparation for global proteome analysis
  - DIA-MS for global proteome analysis
- QUANTIFICATION AND STATISTICAL ANALYSIS
  - Proteomic data analysis

SUPPLEMENTAL INFORMATION

Supplemental information can be found online at https://doi.org/10.1016/j.chembiol.2024.10.007.

Received: February 9, 2024
Revised: July 27, 2024
Accepted: October 18, 2024
Published: November 12, 2024

REFERENCES

1. Békés, M., Langley, D.R., and Crews, C.M. (2022). PROTAC targeted protein degraders: the past is prologue. Nat. Rev. Drug Discov. *21*, 181–200. https://doi.org/10.1038/s41573-021-00371-6.
2. Chamberlain, P.P., and Hamann, L.G. (2019). Development of targeted protein degradation therapeutics. Nat. Chem. Biol. *15*, 937–944. https://doi.org/10.1038/s41589-019-0362-y.
3. Zhao, L., Zhao, J., Zhong, K., Tong, A., and Jia, D. (2022). Targeted protein degradation: mechanisms, strategies and application. Signal Transduct. Target. Ther. *7*, 113. https://doi.org/10.1038/s41392-022-00966-4.
4. Ito, T., Ando, H., Suzuki, T., Ogura, T., Hotta, K., Imamura, Y., Yamaguchi, Y., and Handa, H. (2010). Identification of a Primary Target of Thalidomide Teratogenicity. Science *327*, 1345–1350. https://doi.org/10.1126/science.1177319.
5. Krönke, J., Udeshi, N.D., Narla, A., Grauman, P., Hurst, S.N., McConkey, M., Svinkina, T., Heckl, D., Comer, E., Li, X., et al. (2014). Lenalidomide causes selective degradation of IKZF1 and IKZF3 in multiple myeloma cells. Science *343*, 301–305. https://doi.org/10.1126/science.1244851.
6. Lu, G., Middleton, R.E., Sun, H., Naniong, M., Ott, C.J., Mitsiades, C.S., Wong, K.-K., Bradner, J.E., and Kaelin, W.G. (2014). The Myeloma Drug Lenalidomide Promotes the Cereblon-Dependent Destruction of Ikaros Proteins. Science *343*, 305–309. https://doi.org/10.1126/science.1244917.
7. Chirnomas, D., Hornberger, K.R., and Crews, C.M. (2023). Protein degraders enter the clinic — a new approach to cancer therapy. Nat. Rev. Clin. Oncol. *20*, 265–278. https://doi.org/10.1038/s41571-023-00736-3.
8. Mullard, A. (2021). Targeted protein degraders crowd into the clinic. Nat. Rev. Drug Discov. *20*, 247–250. https://doi.org/10.1038/d41573-021-00052-4.
9. Hanzl, A., and Winter, G.E. (2020). Targeted protein degradation: current and future challenges. Curr. Opin. Chem. Biol. *56*, 35–41. https://doi.org/10.1016/j.cbpa.2019.11.012.
10. Geiger, T.M., Schäfer, S.C., Dreizler, J.K., Walz, M., and Hausch, F. (2022). Clues to molecular glues. Curr. Res. Chem. Biol. *2*, 100018. https://doi.org/10.1016/j.crchbi.2021.100018.
11. Gerry, C.J., and Schreiber, S.L. (2020). Unifying principles of bifunctional, proximity-inducing small molecules. Nat. Chem. Biol. *16*, 369–378. https://doi.org/10.1038/s41589-020-0469-1.
12. Hanzl, A., Barone, E., Bauer, S., Yue, H., Nowak, R.P., Hahn, E., Pankevich, E.V., Koren, A., Kubicek, S., Fischer, E.S., and Winter, G.E. (2023). E3-Specific Degrader Discovery by Dynamic Tracing of Substrate Receptor Abundance. J. Am. Chem. Soc. *145*, 1176–1184. https://doi.org/10.1021/jacs.2c10784.
13. Mayor-Ruiz, C., Bauer, S., Brand, M., Kozicka, Z., Siklos, M., Imrichova, H., Kaltheuner, I.H., Hahn, E., Seiler, K., Koren, A., et al. (2020). Rational discovery of molecular glue degraders via scalable chemical profiling. Nat. Chem. Biol. *16*, 1199–1207. https://doi.org/10.1038/s41589-020-0594-x.
14. Ng, A., Offensperger, F., Cisneros, J.A., Scholes, N.S., Malik, M., Villanti, L., Rukavina, A., Ferrada, E., Hannich, J.T., Koren, A., et al. (2023). Discovery of Molecular Glue Degraders via Isogenic Morphological Profiling. ACS Chem. Biol. *18*, 2464–2473. https://doi.org/10.1021/acschembio.3c00598.
15. Meissner, F., Geddes-McAlister, J., Mann, M., and Bantscheff, M. (2022). The emerging role of mass spectrometry-based proteomics in drug discovery. Nat. Rev. Drug Discov. *21*, 637–654. https://doi.org/10.1038/s41573-022-00409-3.
16. Sathe, G., and Sapkota, G.P. (2023). Proteomic approaches advancing targeted protein degradation. Trends Pharmacol. Sci. *44*, 786–801. https://doi.org/10.1016/j.tips.2023.08.007.
17. Scholes, N.S., Mayor-Ruiz, C., and Winter, G.E. (2021). Identification and selectivity profiling of small-molecule degraders via multi-omics approaches. Cell Chem. Biol. *28*, 1048–1060. https://doi.org/10.1016/j.chembiol.2021.03.007.
18. Mitchell, D.C., Kuljanin, M., Li, J., Van Vranken, J.G., Bulloch, N., Schweppe, D.K., Huttlin, E.L., and Gygi, S.P. (2023). A proteome-wide atlas of drug mechanism of action. Nat. Biotechnol. *41*, 845–857. https://doi.org/10.1038/s41587-022-01539-0.
19. Kozicka, Z., Suchyta, D.J., Focht, V., Kempf, G., Petzold, G., Jentzsch, M., Zou, C., Di Genua, C., Donovan, K.A., Coomar, S., et al. (2024). Design principles for cyclin K molecular glue degraders. Nat. Chem. Biol. *20*, 93–102. https://doi.org/10.1038/s41589-023-01409-z.
20. Liao, H., Liu, X.J., Blank, J.L., Bouck, D.C., Bernard, H., Garcia, K., and Lightcap, E.S. (2011). Quantitative proteomic analysis of cellular protein modulation upon inhibition of the NEDD8-activating enzyme by MLN4924. Mol. Cell. Proteomics *10*. M111.009183. https://doi.org/10.1074/mcp.M111.009183.
21. Savitski, M.M., Zinn, N., Faelth-Savitski, M., Poeckel, D., Gade, S., Becher, I., Muelbaier, M., Wagner, A.J., Strohmer, K., Werner, T., et al. (2018). Multiplexed Proteome Dynamics Profiling Reveals Mechanisms Controlling Protein Homeostasis. Cell *173*, 260–274.e25. https://doi.org/10.1016/j.cell.2018.02.030.
22. Pei, J., Xiao, Y., Liu, X., Hu, W., Sobh, A., Yuan, Y., Zhou, S., Hua, N., Mackintosh, S.G., Zhang, X., et al. (2023). Piperlongumine conjugates induce targeted protein degradation. Cell Chem. Biol. *30*, 203–213.e17. https://doi.org/10.1016/j.chembiol.2023.01.004.
23. Matyskiela, M.E., Lu, G., Ito, T., Pagarigan, B., Lu, C.-C., Miller, K., Fang, W., Wang, N.-Y., Nguyen, D., Houston, J., et al. (2016). A novel cereblon modulator recruits GSPT1 to the CRL4(CRBN) ubiquitin ligase. Nature *535*, 252–257. https://doi.org/10.1038/nature18611.
24. Powell, C.E., Du, G., Che, J., He, Z., Donovan, K.A., Yue, H., Wang, E.S., Nowak, R.P., Zhang, T., Fischer, E.S., and Gray, N.S. (2020). Selective Degradation of GSPT1 by Cereblon Modulators Identified via a Focused

Combinatorial Library. ACS Chem. Biol. *15*, 2722–2730. https://doi.org/10.1021/acschembio.0c00520.

25. Eichelbaum, K., Winter, M., Berriel Diaz, M., Herzig, S., and Krijgsveld, J. (2012). Selective enrichment of newly synthesized proteins for quantitative secretome analysis. Nat. Biotechnol. *30*, 984–990. https://doi.org/10.1038/nbt.2356.
26. Donovan, K.A., Ferguson, F.M., Bushman, J.W., Eleuteri, N.A., Bhunia, D., Ryu, S., Tan, L., Shi, K., Yue, H., Liu, X., et al. (2020). Mapping the Degradable Kinome Provides a Resource for Expedited Degrader Development. Cell *183*, 1714–1731.e10. https://doi.org/10.1016/j.cell.2020.10.038.
27. Kozicka, Z., and Thomä, N.H. (2021). Haven't got a glue: Protein surface variation for the design of molecular glue degraders. Cell Chem. Biol. *28*, 1032–1047. https://doi.org/10.1016/j.chembiol.2021.04.009.
28. Bradner, J., Roberts, J., Nabet, B., Winter, G., Phillips, A.J., Heffernan, T.P., and Buckley, D. (2017). Targeted Protein Degradation to Attenuate Adoptive T-Cell Therapy Associated Adverse Inflammatory Responses (Patent Publication Number: WO-2017024318-A1).
29. An, J., Ponthier, C.M., Sack, R., Seebacher, J., Stadler, M.B., Donovan, K.A., and Fischer, E.S. (2017). pSILAC mass spectrometry reveals ZFP91 as IMiD-dependent substrate of the CRL4CRBN ubiquitin ligase. Nat. Commun. *8*, 15398. https://doi.org/10.1038/ncomms15398.
30. Tsuruyama, T., Imai, Y., Takeuchi, H., Hiratsuka, T., Maruyama, Y., Kanaya, K., Kaszynski, R., Jin, G., Okuno, T., Ozeki, M., et al. (2010). Dual retrovirus integration tagging: identification of new signaling molecules Fiz1 and Hipk2 that are involved in the IL-7 signaling pathway in B lymphoblastic lymphomas. J. Leukoc. Biol. *88*, 107–116. https://doi.org/10.1189/jlb.1109748.
31. Wolf, I., and Rohrschneider, L.R. (1999). Fiz1, a Novel Zinc Finger Protein Interacting with the Receptor Tyrosine Kinase Flt3. J. Biol. Chem. *274*, 21478–21484. https://doi.org/10.1074/jbc.274.30.21478.
32. Mali, R.S., Peng, G.-H., Zhang, X., Dang, L., Chen, S., and Mitton, K.P. (2008). FIZ1 is part of the regulatory protein complex on active photoreceptor-specific gene promoters in vivo. BMC Mol. Biol. *9*, 87. https://doi.org/10.1186/1471-2199-9-87.
33. Mitton, K.P., Swain, P.K., Khanna, H., Dowd, M., Apel, I.J., and Swaroop, A. (2003). Interaction of retinal bZIP transcription factor NRL with Flt3-interacting zinc-finger protein Fiz1: possible role of Fiz1 as a transcriptional repressor. Hum. Mol. Genet. *12*, 365–373. https://doi.org/10.1093/hmg/ddg035.
34. Larivière, N., Law, J., and Trinkle-Mulcahy, L. (2014). Dissection of a Novel Autocrine Signaling Pathway via Quantitative Secretome and Interactome Mapping. J. Proteome Res. *13*, 3432–3443. https://doi.org/10.1021/pr500392m.
35. McShane, E., Sin, C., Zauber, H., Wells, J.N., Donnelly, N., Wang, X., Hou, J., Chen, W., Storchova, Z., Marsh, J.A., et al. (2016). Kinetic Analysis of Protein Stability Reveals Age-Dependent Degradation. Cell *167*, 803–815.e21. https://doi.org/10.1016/j.cell.2016.09.015.
36. Takahashi, D., Moriyama, J., Nakamura, T., Miki, E., Takahashi, E., Sato, A., Akaike, T., Itto-Nakama, K., and Arimoto, H. (2019). AUTACs: Cargo-Specific Degraders Using Selective Autophagy. Mol. Cell *76*, 797–810.e10. https://doi.org/10.1016/j.molcel.2019.09.009.
37. Banik, S.M., Pedram, K., Wisnovsky, S., Ahn, G., Riley, N.M., and Bertozzi, C.R. (2020). Lysosome-targeting chimaeras for degradation of extracellular proteins. Nature *584*, 291–297. https://doi.org/10.1038/s41586-020-2545-9.
38. Henning, N.J., Boike, L., Spradlin, J.N., Ward, C.C., Liu, G., Zhang, E., Belcher, B.P., Brittain, S.M., Hesse, M.J., Dovala, D., et al. (2022). Deubiquitinase-targeting chimeras for targeted protein stabilization. Nat. Chem. Biol. *18*, 412–421. https://doi.org/10.1038/s41589-022-00971-2.
39. Iconomou, M., and Saunders, D.N. (2016). Systematic approaches to identify E3 ligase Substrates. Biochem. J. *473*, 4083–4101. https://doi.org/10.1042/BCJ20160719.
40. Kleinpenning, F., Steigenberger, B., Wu, W., and Heck, A.J.R. (2020). Fishing for newly synthesized proteins with phosphonate-handles. Nat. Commun. *11*, 3244. https://doi.org/10.1038/s41467-020-17010-0.
41. Derks, J., Leduc, A., Wallmann, G., Huffman, R.G., Willetts, M., Khan, S., Specht, H., Ralser, M., Demichev, V., and Slavov, N. (2023). Increasing the throughput of sensitive proteomics by plexDIA. Nat. Biotechnol. *41*, 50–59. https://doi.org/10.1038/s41587-022-01389-w.
42. Borteçen, T., Müller, T., and Krijgsveld, J. (2023). An integrated workflow for quantitative analysis of the newly synthesized proteome. Nat. Commun. *14*, 8237. https://doi.org/10.1038/s41467-023-43919-3.
43. Perez-Riverol, Y., Bai, J., Bandla, C., García-Seisdedos, D., Hewapathirana, S., Kamatchinathan, S., Kundu, D.J., Prakash, A., Frericks-Zipper, A., Eisenacher, M., et al. (2022). The PRIDE database resources in 2022: a hub for mass spectrometry-based proteomics evidences. Nucleic Acids Res. *50*, D543–D552. https://doi.org/10.1093/nar/gkab1038.
44. Cox, J., and Mann, M. (2008). MaxQuant enables high peptide identification rates, individualized p.p.b.-range mass accuracies and proteome-wide protein quantification. Nat. Biotechnol. *26*, 1367–1372. https://doi.org/10.1038/nbt.1511.
45. Ritchie, M.E., Phipson, B., Wu, D., Hu, Y., Law, C.W., Shi, W., and Smyth, G.K. (2015). limma powers differential expression analyses for RNA-sequencing and microarray studies. Nucleic Acids Res. *43*, e47. https://doi.org/10.1093/nar/gkv007.
46. Hanzl, A., Casement, R., Imrichova, H., Hughes, S.J., Barone, E., Testa, A., Bauer, S., Wright, J., Brand, M., Ciulli, A., and Winter, G.E. (2023). Functional E3 ligase hotspots and resistance mechanisms to small-molecule degraders. Nat. Chem. Biol. *19*, 323–333. https://doi.org/10.1038/s41589-022-01177-2.
47. Schwanhäusser, B., Busse, D., Li, N., Dittmar, G., Schuchhardt, J., Wolf, J., Chen, W., and Selbach, M. (2011). Global quantification of mammalian gene expression control. Nature *473*, 337–342. https://doi.org/10.1038/nature10098.
48. Bruderer, R., Bernhardt, O.M., Gandhi, T., Miladinović, S.M., Cheng, L.-Y., Messner, S., Ehrenberger, T., Zanotelli, V., Butscheid, Y., Escher, C., et al. (2015). Extending the Limits of Quantitative Proteome Profiling with Data-Independent Acquisition and Application to Acetaminophen-Treated Three-Dimensional Liver Microtissues. Mol. Cell. Proteomics *14*, 1400–1410. https://doi.org/10.1074/mcp.M114.044305.

CellPress
OPEN ACCESS

STAR★METHODS

KEY RESOURCES TABLE

REAGENT or RESOURCE	SOURCE	IDENTIFIER
Antibodies		
Rabbit polyclonal α-CyclinK	Bethyl Laboratories	Cat# A301-939A; RRID: AB_1547934
Rabbit monoclonal α-β-Actin	Cell Signaling	Cat# 4970; RRID: AB_2223172
Mouse monoclonal α-Tubulin	GeneTex	Cat# GTX628802; RRID: AB_2716636
Mouse monoclonal α-Vinculin	Santa Cruz	Cat# sc-73614; RRID: AB_1131294
Rabbit polyclonal α-FLAG	Cell Signaling	Cat# #2368; RRID: AB_2217020
Mouse monoclonal α-FLAG	Sigma-Aldrich	Cat# F1804; RRID: AB_262044
Rabbit polyclonal α-IKZF3	Novus Biologicals	Cat# NBP2-24495; RRID: AB_3096994
Rabbit monoclonal α-CRBN	Cell Signaling	Cat #71810; RRID: AB_2799810
Mouse α-rabbit IgG-HRP	Santa Cruz	Cat# sc-2357; RRID: AB_628497
Goat α-rabbit IgG-HRP	Jackson ImmunoResearch	Cat# 111-035-003; RRID: AB_2313567
Mouse IgGκ BP-HRP	Cell Signaling	Cat# sc-516102; RRID: AB_2687626
Chemicals, peptides, and recombinant proteins		
MLN4924	THP Medical	Cat# HY-70062
Carfilzomib	Selleck Chemicals	Cat# S2852
TAK243	MedChem Express	Cat# HY-100487
CC220	Selleck Chemicals	Cat# S8760
CC122	Selleck Chemicals	Cat# S7892
Thalidomide	Sigma-Aldrich	Cat# T144
Lenalidomide	Sigma-Aldirch	Cat# SML2283
Pomalidomide	THP Medical	Cat# HY-10984
CC-885	MedChem Express	Cat# HY-101488
CC-90009	MedKoo	Cat# 207005
dialyzed FBS	Gibco	Cat# 26400-044
GlutaMAX	Gibco	Cat# 35050061
SILAC-intermediate L-lysine	Silantes	Cat# 211103913
SILAC-intermediate L-arginine	Silantes	Cat# 201203902
SILAC-heavy L-lysine	Silantes	Cat# 211604102
SILAC-heavy L-arginine	Silantes	Cat# 201604102
SILAC-RPMI 1640	AthenaES	Cat# AES-0432
L-azidohomoalanine	Click Chemistry Tools	Cat# 1066-1000
L-lysine	Sigma	Cat# L8662-100G
L-Arginine	Sigma	Cat# A8094-100G
Pen-Strep	Gibco	Cat# 15140-122
sodium pyruvate	Gibco	Cat# 11360070
NP-40	Sigma	Cat# 74385-1L
Na-Deoxycholate	Sigma-Aldrich	Cat# D6750-25G
CHAPS	Serva	Cat# 17038.04
SDS	Bio-Rad	Cat# 1610418
cOmplete protease inhibitor	Roche	Cat# 11873580001
Laemmli Sample Buffer	Bio-Rad	Cat# 1610747
DTT	Biomol	Cat# 04010.25
Clarity Western ECL Substrate	Bio-Rad	Cat# 1705061
Clarity Max Western ECL Substrate	Bio-Rad	Cat# 1705062
Endurazine Luciferase live cell substrate	Promega	Cat# N2570

(*Continued on next page*)

Continued

REAGENT or RESOURCE	SOURCE	IDENTIFIER
Trypsin/LysC	Promega	Cat# V5073
RapiGest	Waters	Cat# 186001861
TCEP	Sigma	Cat# C4706-10G
Critical commercial assays		
BCA Protein Assay	Thermo Scientific	Cat# 23225
Rapid Gold BCA Protein Assay	Thermo Scientific	Cat# A53225PR
Click-iT Protein Enrichment Kit	Invitrogen	Cat# C10416
Quantitative Colorimetric Peptide Assay	Thermo Scientific	Cat# 23275
Deposited data		
Proteomics data	This paper	https://www.ebi.ac.uk/pride/archive/projects/PXD048931
Experimental models: Cell lines		
Human KBM7	Thijn Brummelkamp lab, NKI Amsterdam	N/A
Human Jurkat	Jay Bradner Lab, Harvard	N/A
Human HEK293T	Jay Bradner Lab, Harvard	N/A
Human RKO	ATCC	Cat# CRL-2577
Recombinant DNA		
VSV.G	Addgene	Cat# 14888
psPAX2	Addgene	Cat# 12260
pLEX305	Addgene	Cat# 41390
Software and algorithms		
MaxQuant v1.6.0.16	Cox and Mann[44]	https://cox-labs.github.io/coxdocs/Download_Installation.html
R project	N/A	https://www.r-project.org/
limma package v.3.44.3	Ritchie et al.[45]	https://bioconductor.org/packages/release/bioc/html/limma.html
Spectronaut v15.1.210713	Biognosis	N/A
Other		
Orbitrap Fusion Tribrid mass spectrometer	Thermo Scientific	N/A
Q Exactive HF mass spectrometer	Thermo Scientific	N/A
Easy-nLC1200 system	Thermo Scientific	N/A
Infinity 1260 LC system	Agilent	N/A
Gemini C18 3 μmparticle-size column	Phenomonex	Cat# 00D-4439-A0
Acclaim Pepmap C18 5 μm-particle-size trap column	Thermo Scientific	Cat# 164564-CMD
nanoEase M/Z Peptide BEH C18 column	Waters	Cat# 186008795
Oasis PRiME HKB μElution Plate	Waters	Cat# 186008052

EXPERIMENTAL MODEL AND STUDY PARTICIPANT DETAILS

Cell culture

All cells were cultured at 37°C in a humidified 5% CO2-atmosphere. Unlabeled KBM7 cells were maintained in Iscove's Modified Dulbecco's Medium supplemented with 10% (v/v) FBS and 1× Pen-Strep (Gibco #15140-122). Unlabeled Jurkat cells were maintained in Roswell Park Memorial Institute (RPMI) 1640 medium supplemented with 10% (v/v) FBS and 1× Pen-Strep. HEK293 cells (a gift by the Bradner Lab) were maintained in Dulbecco's Modified Eagle Medium (DMEM) supplemented with 10% (v/v) FBS and 1× Pen-Strep. SILAC-intermediate labeled KBM7 and Jurkat cells were maintained in RPMI 1640 for SILAC (Thermo Scientific #A33823) supplemented with 10% (v/v) dialyzed FBS (dFBS, Gibco #26400-044), 1× Pen-Strep, 200 mg/L L-proline, 1× GlutaMAX (Gibco #35050061), 200 mg/L SILAC-intermediate L-lysine (Silantes #211103913) and 40 mg/L SILAC-intermediate L-arginine (Silantes #201203902).

CellPress
OPEN ACCESS

METHOD DETAILS

Lentivirus production and generation of stable cell lines

For lentiviral production, HEK293T cells were seeded in 6-well plates and transfected at approx. 80% confluency with 0.69 μg target vector, 0.17 μg VSV.G (Addgene #14888) and 0.34 μg psPAX2 (Addgene #12260) using PEI following standard protocol. 72 h later, supernatant containing virus was harvested, centrifuged at 2000 rpm for 5 min to remove cell debris. Lentivirus was then aliquoted and stored at – 80°C until transduction of 0.25 × 10^6 cells in 1 mL of media plus virus in 24 well plates with the addition of 8 μg/mL polybrene (Sigma) and spin inoculation for 1 h at 2,000 r.p.m. Antibiotic selection was performed 24 h after transduction with 1 μg/mL puromycin. For overexpression of IKZF3 and FIZ1, full-length IKZF3 and FIZ1 was synthesized by Genscript and cloned into a modified pLEX305 backbone harboring a nluc-3x-FLAG tag via Gateway cloning (Thermo Fisher Scientific) following manufacturer's recommendations. Monoclonal CRBN knockout RKO cells with and without reconstituted wild-type CRBN, generated as described before,[46] were transduced with a lentiviral plasmid for stable expression of FIZ1-NanoLuc-3xFlag and selected with 1 μg/mL Puromycin. Cells were seeded into 12-well plates. The following day, cells were treated with DMSO or 10 μM of IMiDs (Compound 1, CC-90009, or pomalidomide). After 24 h of treatment, cells were harvested for western blot analysis.

Small-molecule degraders

MLN4924 (THP Medical #HY-70062), Carfilzomib (Selleck Chemicals #S2852), TAK243 (MedChem Express #HY-100487), CC220 (Selleck Chemicals #S8760), CC122 (Selleck Chemicals #S7892), Thalidomide (Sigma-Aldrich #T144), Lenalidomide (Sigma-Aldirch #SML2283), Pomalidomide (THP Medical Product #HY-10984), CC-885 (MedChem Express #HY-101488), CC-90009 (MedKoo #207005).

Synthesis of compound 1

Reactions were monitored by thin-layer chromatography using pre-coated silica gel plates F-254. Proton nuclear magnetic resonance (^{1}H NMR) spectra and carbon nuclear magnetic resonance (^{13}C NMR) spectra were recorded on Bruker AV III 600 instrument from the NMR Facility of the University of Vienna. The NMR peak multiplicities are denoted as follows: s, singlet; d, doublet; dd, doublet of doublets; m, multiplet. Column chromatography was carried out using Biotage Selekt over Biotage Sfar Silica D column cartridges employing Merck silica gel (Kieselgel 60, 63–200 mm). HRMS (ESI-TOF) analyses were performed on Bruker timsTOF flex at the MS Facility of the University of Vienna.

A mixture of 2-(2,6-dioxopiperidin-3-yl)-4-fluoroisoindoline-1,3-dione (20 mg, 0.0724 mmol, 1.0 eq.), cyclopropylamine (0.080 mmol, 1.1 eq.) and DIPEA (0.141 mmol, 1.9 eq.) in N-methylpyrrolidinone (0.1 M) was heated to 90°C overnight. The reaction mixture was cooled to room temperature and diluted in ethyl acetate. The organic layer was washed with saturated solution of NaHCO3, water and brine, and subsequently dried over anhydrous sodium sulfate and concentrated under reduced pressure. The residue was purified by flash column chromatography on silica gel using dichloromethane/methanol as solvent system to afford the title compound as a yellow powder.

4-(cyclopropylamino)-2-(2,6-dioxopiperidin-3-yl)isoindoline-1,3-dione. 22 mg. Yield 70%. Characterization data correspond to previously reported. ^{1}H NMR (600 MHz, DMSO) δ 11.09 (s, 1H), 7.65 (dd, J = 8.5, 7.1 Hz, 1H), 7.36 (d, J = 8.5 Hz, 1H), 7.16–7.07 (m, 1H), 6.64 (d, J = 2.0 Hz, 1H), 5.05 (dd, J = 12.9, 5.5 Hz, 1H), 2.95–2.82 (m, 1H), 2.62–2.56 (m, 2H), 2.55–2.46 (m, 1H), 2.07–1.97 (m, 1H), 0.86–0.79 (m, 2H), 0.61–0.52 (m, 2H). ^{13}C NMR (151 MHz, DMSO) δ 172.8, 170.0, 168.7, 167.3, 146.8, 136.1, 132.0, 118.3, 111.3, 109.7, 48.5, 30.9, 24.1, 22.1, 7.3. HRMS (ESI) $[M + H]^+$ calcd for C16H15N3O4, 314.1135, found 314.1136.

Western blot

Cells were harvested into ice-cold PBS, pelleted, and resuspended in RIPA lysis buffer containing 50 mM Tris-HCl pH 7.5, 1% (v/v) NP-40, 0.25% (w/v) Na-Deoxycholate, 0.1% (w/v) SDS, 150 mM NaCl, 1 mM EDTA, 10% (v/v) glycerol and 1× Halt (1:100, Thermo Scientific, 78429) or 1× cOmplete EDTA-free protease inhibitor cocktail (Roche #11873580001). Lysates were sonicated with a probe sonicator and cleared via centrifugation at 15,000 × g for 5 min at 4°C. Protein concentrations were measured with either the Pierce BCA Protein Assay Kit (Thermo Scientific #23225) or the Pierce Rapid Gold BCA Protein Assay Kit (Thermo Scientific #A53225PR). One part of cleared lysate was combined with three parts of 4× Laemmli Sample Buffer (Bio-Rad #1610747) containing 400 mM DTT. Samples were heated to 90°C for 10 min, vortexed and cooled down to room temperature. Equal protein amounts were loaded onto 4–15% Mini-PROTEAN TGX Precast Protein Gels (Bio-Rad #4561086DC) or a Bolt 4–12% Bis-Tris Plus Wedgewell Gel submerged in 1× TGS-Buffer (Bio-Rad #1610772). Precision Plus Protein Dual Color Standard (Bio-Rad #4561084DC) was loaded as a molecular weight reference and the electrophoresis performed until the dye reached the end of the gel. Proteins were transferred onto an Amersham Hybond 0.45 μm PVDF Blotting Membrane (Cytiva #15259894). Standard Western Blot analysis was performed using primary antibodies against Cyclin K (1:5000, Bethyl Laboratories #A301-939A), β-Actin (1:4000, Cell Signaling #4970), α-Tubulin (1:2000, GeneTex #GT114), Flag (DYKDDDDK, 1:1000, CellSignaling #2368 (Figures 4D and 4E); or 1:1000, Sigma-Aldrich, F1804 (Figure 4H)), IKZF3 (1:1000, Novus Biologicals #NBP2-24495), CRBN (1:1000, Cell Signaling Technology, 71810S)), and Vinculin (1:1000, Santa Cruz Biotechnology, sc-73614). Anti-rabbit IgG-HRP (1:10000, Santa Cruz Biotechnology #sc-2357 or Jackson ImmunoResearch #111-035-003) and anti-rabbit IgG-HRP (1:10000, Santa Cruz Biotechnology #sc-516102) were used for enhanced chemiluminescence detection with either Clarity Western ECL Substrate (Bio-Rad #1705061) or Clarity Max Western ECL Substrate (Bio-Rad #1705062).

Luminescence assay

For NanoLuc measurements, 10000 cells in 30 μL media were seeded into each well of a black 384-well plate (Corning #3764). 1:100 Endurazine Luciferase live cell substrate (Promega) were added to each well, followed by a 60 min incubation. At time point 0, 10 μL of pre-made compound solution in media was added to each well and luciferase measurements were performed on an EnVision plate reader (PerkinElmer).

Pulsed-SILAC-AHA labeling for degradome analysis

Fully SILAC-intermediate labeled KBM7 or Jurkat cells were seeded into RPMI SILAC-intermediate medium and grown overnight. The next day, the old media was removed and the cells were washed with warm PBS two times. Cells were deprived of methionine by incubating them for 1 h in methionine-free depletion medium consisting of SILAC-RPMI 1640 (AthenaES #AES-0432) supplemented with 10% (v/v) dFBS, 10 mM HEPES, 1 mM sodium pyruvate (Gibco #11360070), 300 mg/L L-proline, 50 mg/L L-leucine and 1× GlutaMAX (Gibco #35050061). After removal of the depletion medium, half of the cells were pulse-labeled in AHA-SILAC-heavy medium consisting of depletion media additionally supplemented with 200 mg/L SILAC-heavy L-lysine (Silantes #211604102), 40 mg/L SILAC-heavy L-arginine (Silantes #201604102) and 0.1 mM L-azidohomoalanine (Click Chemistry Tools #1066-1000). The other half of the cells were labeled in AHA-SILAC-light medium containing regular L-lysine, regular L-arginine and L-azidohomoalanine at the same concentrations as the heavy media. After 8 h of AHA-SILAC-pulse labeling, cells were transferred into RPMI SILAC-intermediate medium again and divided into multiple smaller cultures (one 10 cm dish per timepoint, replicate and SILAC-channel). The heavy-pulsed cells were treated with the drug of interest for the indicated amount of time, while the light-pulsed cells were treated with DMSO. Cells were harvested by centrifugation, washed with ice-cold PBS and pellets stored at −20°C until lysis. All experiments were performed in triplicate.

Pulsed SILAC-AHA labeling for translatome analysis

Fully SILAC-intermediate labeled Jurkat cells were seeded into RPMI SILAC-intermediate medium and grown overnight. The next day, the old medium was removed and the cells were washed with warm PBS two times. Cells were deprived of methionine by incubating them for 1 h in methionine-free depletion medium consisting of SILAC-RPMI 1640 (AthenaES #AES-0432) supplemented with 10% (v/v) dFBS, 10 mM HEPES, 1 mM sodium pyruvate (Gibco #11360070), 300 mg/L L-proline, 50 mg/L L-leucine and 1× GlutaMAX (Gibco #35050061). After removal of the depletion medium, half of the cells were subjected to AHA-SILAC-heavy medium consisting of depletion media additionally supplemented with 200 mg/L SILAC-heavy L-lysine (Silantes #211604102), 40 mg/L SILAC-heavy L-arginine (Silantes #201604102) and 0.1 mM L-azidohomoalanine (Click Chemistry Tools #1066-1000), while the other half of the cells were subjected to AHA-SILAC-light medium containing regular L-lysine, regular L-arginine and L-azidohomoalanine at the same concentrations as the heavy media. Cells were divided into multiple smaller cultures (one 10 cm dish per timepoint, replicate and SILAC-channel) and the heavy-pulsed cells were treated with the drug of interest for the indicated amount of time, while the light-pulsed cells were treated with DMSO. Cells were harvested by centrifugation, washed with ice-cold PBS and pellets stored at −20°C until lysis. All experiments were performed in triplicate.

Click-iT protein enrichment, reduction, alkylation and digestion

Cell pellets from pulsed-SILAC-AHA experiments were resuspended in urea lysis buffer consisting of 200 mM HEPES pH 8, 0.5 M NaCl, 4% (w/v) CHAPS, 8 M Urea and 1× cOmplete EDTA-free protease inhibitor (Roche #11873580001). Lysates were sonicated with a probe sonicator and cleared via centrifugation at 15,000 × g for 30 min. Protein concentrations were measured with either the Pierce BCA Protein Assay Kit (Thermo Scientific #23225) or the Pierce Rapid Gold BCA Protein Assay Kit (Thermo Scientific #A53225PR). Equal protein amounts of corresponding SILAC-pairs were combined to a total of 3 mg. AHA-labeled proteins were enriched with the Click-iT Protein Enrichment Kit (Invitrogen #C10416). For this, 100–120 μL of resin were washed with water two times in order to remove the storage solution. The beads were resuspended in 100 μL water, combined with the lysate and the volume adjusted to 1.9 mL with urea lysis buffer. To start the Click-iT reaction, 10 μL of 200 mM Cu(II)SO_4, 62.5 μL of 160 mM reaction additive 1 and 10 μL of 2 M reaction additive 2 (All components from the Click-iT Protein Enrichment Kit) were combined and added to each sample. Samples were then incubated at 40°C for 2 h while shaking, leading to the covalent capture of AHA-labeled proteins to the alkyne-activated resin. The beads were washed with water two times and resuspended in 100 μL water. In order to reduce and alkylate proteins bound to the beads, 2 mL SDS-wash buffer (Click-iT Protein Enrichment Kit) supplemented with 1 mM TCEP and 0.25 mM Chloroacetamide were added to each sample. Samples were then incubated at 70°C for 15 min while shaking at 1,800 rpm in an orbital shaker, followed by 15 min incubation at room temperature, also shaking at 1,800 rpm. Resins were transferred into a spin column (Click-iT Protein Enrichment Kit) and stringently washed with 2 mL water, 5 × 2 mL SDS-wash buffer (Click-iT Protein Enrichment Kit), 2 mL water, 5 × 2 mL guanidine wash buffer (100 mM Tris-HCL pH 8, 6 M Guanidine-HCl) and 5 × 2 mL 20% (v/v) acetonitrile (ACN). The resin was resuspended in 2 mL digestion buffer (100 mM Tris-HCl pH8, 5% (v/v) ACN, 2 mM $CaCl_2$) and pelleted by centrifugation. 1.8 mL of digestion buffer was removed, leaving the beads in 200 μL, and 10 μL of 0.1 μg/μL Trypsin/LysC Mix (Promega #V5073) was added. Proteins were digested at 37°C overnight while shaking at 1,000 rpm in an orbital shaker. To retrieve the tryptic peptides, the resin was pelleted and the supernatant transferred to a fresh tube. The resin was resuspended in 600 μL water, vortexed, pelleted and the supernatant added to the previous tube (=800 μL total). Samples were acidified by adding formic acid (FA) to 1% (v/v) and cleaned up via reversed-phase solid phase extraction with an Oasis PRiME HKB μElution Plate (Waters #186008052) following the instructions. Eluates were dried in a centrifugal evaporator and resuspended in

0.1% (v/v) FA. If peptide concentrations were measured, the Pierce Quantitative Colorimetric Peptide Assay (Thermo Scientific, #23275) was used. Peptides were then fractionated via high-pH reversed-phase fractionation.

High-pH reversed-phase fractionation

Samples were fractionated using an Infinity 1260 LC system (Agilent) with a Gemini C_{18} 3 μm-particle-size column (1 × 100 mm, Phenomonex #00D-4439-A0). An alkaline water/ACN gradient with a flow rate of 0.1 mL/min was used for elution. Solvent A contained 20 mM ammonium formate in H_2O at pH 10 and solvent B was 100% ACN. The following gradient profile was used: 0–2 min 0% B, 2–60 min linear gradient to 65% B, 60–62 min linear gradient to 85% B, 62–67 min 85% B, 67–85 min 100% B. Eluting samples were either collected in 60 fractions and concatenated to 12 fractions or collected in 40 fractions and concatenated to 8 fractions. Samples were dried in a centrifugal evaporator and resuspended in 1% (v/v) FA. All fractions were cleaned up via reversed-phase solid phase extraction with an Oasis PRiME HKB μElution Plate (Waters #186008052) following the instructions. Eluates were dried in a centrifugal evaporator and resuspended in 0.1% (v/v) FA, followed by DDA-MS.

DDA-MS for degradome and translatome analysis

An Easy-nLC1200 system (Thermo Scientific) connected to an Orbitrap Fusion Tribrid MS (Thermo Scientific) was used for DDA proteomics analysis. Peptides were loaded onto an Acclaim Pepmap C_{18} 5 μm-particle-size trap column (0.1 × 20 mm, Thermo Scientific #164564-CMD) and separated over a nanoEase M/Z Peptide BEH C_{18} 1.7 μm-particle-size analytical column (0.075 × 250 mm, Waters #186008795) which was heated to 55°C. Peptides were resolved with a water/ACN gradient consisting of solvent A (0.1% (v/v) FA in H_2O) and solvent B (0.1% (v/v) FA and 80% (v/v) ACN in H_2O). The following gradient profile was used with a flow rate of 300 nL/min: 0–2.8 min 3.7% B, 2.8–50 min linear gradient to 33.9% B, 50–58 min linear gradient to 52.4% B, 58–58.1 min linear gradient to 83.2% B, 58.1–74 min 83.2% B, 74–75 min linear gradient to 3.7% B, 75–105 min 3.7% B. Eluted ions were injected by electrospray ionization (ESI) and analyzed by MS/MS. The ion transfer tube temperature was set to 320°C and MS1 was performed at a resolution of 60,000 within the range of 375–1500 m/z. The automatic gain control (AGC) target was set to 1×10^6 and the maximum injection time to 50 ms. The most abundant ions with a charge between 2 and 4 were selected from a 3 s cycle time window. Dynamic exclusion was set to 20 s with a mass tolerance of + -10 ppm. MS2 occurred with a higher-energy collisional dissociation of 33% and an isolation window of 1.6 m/z. The AGC target was set to 1×10^4 and the maximum injection time to 50 ms.

Sample preparation for global proteome analysis

Unlabeled Jurkat cells were treated for 8 h either with 100 nM CC-885 or DMSO, harvested by centrifugation and washed with ice-cold PBS. Cell pellets were lysed in 0.1% RapiGest buffer (0.1% RapiGest in 100 mM Ammonium bicarbonate, 40 mM TCEP and 40 mM Chloroacetamide) and sonicated using a probe sonicator. Protein concentrations were determined from cleared lysates with either the Pierce BCA Protein Assay Kit (Thermo Scientific #23225) or the Pierce Rapid Gold BCA Protein Assay Kit (Thermo Scientific #A53225PR). 100 μg of protein was digested overnight at 37°C using Trypsin/LysC. On the next day, digestion was stopped by adding TFA to a final concentration of 1% (v/v). Samples were then incubated at 37°C for 30 min and centrifuged at 16000 × g and 4°C for additional 30 min. Cleared supernatants were collected and analyzed by data independent acquisition (DIA)-MS.

DIA-MS for global proteome analysis

An Easy-nLC1200 system (Thermo Scientific) connected to a Q Exactive HF MS (Thermo Scientific) was used for DIA proteomic analysis. Peptides were loaded onto an Acclaim Pepmap C_{18} 5 μm-particle-size trap column (0.1 × 20 mm, Thermo Scientific #164564-CMD) and separated over a nanoEase M/Z Peptide BEH C_{18} 1.7 μm-particle-size analytical column (0.075 × 250 mm, Waters #186008795) which was heated to 55°C. Peptides were resolved with a water/ACN gradient consisting of solvent A (0.1% (v/v) FA in H_2O) and solvent B (0.1% (v/v) FA and 80% (v/v) ACN in H_2O). The following gradient profile was used with a flow rate of 300 nL/min: 0–3 min 2% B, 3–153 min linear gradient to 25% B, 153–183 min linear gradient to 40% B, 183–184 min linear gradient to 95% B, 184–189 min 95% B, 189–190 min linear gradient to 2% B, 190–210 min 2% B. Eluted ions were injected by electrospray ionization (ESI) and analyzed by MS/MS. The ion transfer tube temperature was set to 320°C and MS1 was performed at a resolution of 60,000 within the range of 400–1200 m/z. The AGC target was set to 3×10^6 and the maximum injection time to 20 ms. Data-independent MS/MS spectra were acquired at an Orbitrap resolution of 30,000, an AGC target of 3×10^6 and an automated maximum injection time using 34 non-overlapping isolation windows of 24.3 m/z. The normalized collision energy was set to 27 and the fixed first mass to 200 m/z.

QUANTIFICATION AND STATISTICAL ANALYSIS

Proteomic data analysis

For degradome and translatome analyses, proteins and peptides were identified and quantified from raw spectral files via MaxQuant v1.6.0.16[44] using the UniProt human reference proteome database (Proteome ID: UP000005640) only using 'reviewed' proteins, and the default list of contaminants that is integrated in Andromeda. Masses of SILAC labels, the match-between-runs option and intensity-based absolute quantification[47] were activated in all searches, while remaining settings were used at default. Proteins and peptides that were marked by MaxQuant as contaminants, reverse or only identified by site were excluded from all datasets. The remaining quantified proteins were log2-transformed and median-normalized, which was used as an input for differential protein

analysis in the limma package v.3.44.3 in the R framework.[45] Specifically, limma assesses relative protein expression by fitting a linear model, and empirical Bayes posterior variance estimators to smoothen the standard errors. Robust option was set to true to protect against outlier sample variances. Finally, Benjamini - Hochberg was applied to correct for multiple testing. For global proteome experiments, proteins were identified and quantified via Spectronaut v15.1.210713[48] in directDIA mode using the same UniProt database indicated above. Enzyme specificity was set to Trypsin and LysC, while other settings were left at default. Further statistical analysis was performed in limma as indicated above.